Polarization-gradient laser cooling as a way to create strongly localized structures for atom lithography

O. N. Prudnikov and A. V. Taichenachev
Novosibirsk State University, Pirogova 2, Novosibirsk 630090, Russia

A. M. Tumaikin and V. I. Yudin
Institute of Laser Physics SB RAS, Lavrentyeva 13/3, Novosibirsk 630090, Russia

(Received 26 June 2006; published 28 February 2007)

Generally, conditions for deep sub-Doppler laser cooling do not match conditions for strong atomic localization, that takes place in a deeper optical potential and leads to higher temperature. Moreover, for a given detuning in a deep optical potential the secular approximation, which is frequently used for a quantum description of laser cooling, fails. Here we investigate the atomic localization in optical potential, using a full quantum approach for atomic density matrix beyond the secular approximation. It is shown that laser cooling in a deep optical potential, created by a light field with polarization gradients, can be used as an alternative method for the formation of high contrast spatially localized structures of atoms for the purposes of atom lithography and atomic nanofabrication. Finally, we analyze possible limits for the width and contrast of localized atomic structures that can be reached in this type of light mask.

DOI: 10.1103/PhysRevA.75.023413 PACS number(s): 32.80.Pj, 42.50.Vk

I. INTRODUCTION

Laser cooling and manipulation of neutral atoms is one of the priority field in atomic optics. In recent years great developments and success have been obtained in atom lithography and direct deposition of atoms, utilizing light fields as an immaterial optical mask for atomic beam [1,2]. In most nanofabrication experiments, atomic spatial structures are realized by a periodical conservative potential created by far off detuned intense laser fields acting as an array of immaterial light lenses for atoms. The influence of the spontaneous emission on the focusing is considered to be negligible because of the large light detuning and short interaction times. In essence, atom trajectories are affected by the conservative dipole force without any loses (or dissipation) of energy in an atomic beam. In this case the atomic beam focusing has a classical analogy and can be described with methods developed in particle optics [3,4]. As in classical optics, the feature size is limited by a combination of chromatic aberrations caused by the broad longitudinal and transverse velocity distribution of an atomic beam. Therefore, in order to minimize deleterious effects an additional laser field is required to prepare a well collimated atomic beam by transverse laser cooling. Additionally, because of spherical aberrations some atoms are not well focused and contribute to the pedestal background. These factors are dominant and do not allow one to reach the theoretically predicted diffraction limit for atom optics determined by de Broglie wavelength of atoms. Therefore new alternative methods for atom lithography are intensively investigated.

The idea of combining the traditional focusing method with the well known concept of laser cooling for a blue detuned intensive light field has been suggested in Ref. [5] and was thoroughly studied in Refs. [6,7]. In this case the intensive light field is mainly used for focusing of atomic beam by deep optical potential. Additionally dissipative light force provides cooling of atoms to the minimum of optical potential at blue detunings. The characteristic time when the dissipative processes take effect is a few inverse recoil frequencies ω_R^{-1} (where $\hbar\omega_R=\hbar^2k^2/2M$ is the recoil energy, gained by an atom with mass M at rest after emission of a photon with momentum $\hbar k$). This time is several tens of microseconds for the majority of elements with closed dipole optical transitions suitable for laser cooling. However, for atomic beams with the thermal longitudinal velocity it might be difficult to realize this type of dissipative optical mask experimentally due to power limitations of used laser system.

In the present paper we consider an alternative regime of dissipative optical mask, created by red detuned low intensity light field with spatially inhomogeneous polarization. It is well known that low intensity light fields with polarization gradients can be used for sub-Doppler laser cooling of neutral atoms. On the contrary to laser cooling, where the major purpose is to reach the lowest temperatures of atoms, here we are interested in the strongest spatial atomic localization, while the temperature of atoms is not necessarily low. We consider the steady-state atomic density matrix in the framework of full quantum treatment. In this case the size of atomic localization is a function of the light field parameters only, while for the well known nondissipative light mask this size is determined by the focal-length of light lens [1,4] and by the initial transverse velocity distribution.

We are mainly interested in such regimes of dissipative light masks where the strongest atomic localization is realized. Obviously, the steady-state density matrix is not sensitive to the initial atomic beam momentum distribution. This solution is achieved for the long enough atom-light interaction time (of order of a few ω_R^{-1}). Thus, the main attention is devoted to possible limits for atomic spatial localization that can be achieved in this type of dissipative light mask.

The mechanisms of laser cooling were studied by a number of authors especially with respect to the atomic momentum distribution [8–12]. The effects of spatial localization and quantization have been first observed in one-dimensional

optical lattices [13,14]. Theoretically the spatial atomic localization is usually studied in the secular approximation [11,12,15–18] which is valid in the limit

$$\sqrt{U_0/\hbar\omega_R} \ll |\delta|/\gamma. \tag{1}$$

Here U_0 is the optical potential depth, $\delta=\omega-\omega_0$ is the detuning between the laser ω and atomic transition ω_0 frequencies, and γ is the radiative decay rate. The condition (1) assumes that the energy separations between different energy bands in optical potential are much greater then their width, originating from the optical pumping and tunneling effects. For a given potential depth U_0 this approximation is valid at sufficiently large detuning. Vice versa, it can fail in a deep potential for given detuning. Moreover, even if the secular approximation is well fulfilled for the lower vibrational levels it can break down for upper levels, where the separation between energy bands becomes smaller due to the potential anharmonicity [12]. Certainly, the secular approximation (1) fails for atoms moving above the potential barrier. Therefore, these circumstances make very hard to use the secular approximation for an adequate description of hot and nonlocalized atomic fraction.

In the present work we consider conditions far from the situation of extremely low sub-Doppler cooling. Thus, to describe the localization of atoms correctly we do not restrict our analysis by secular approximation. Rather we perform a full quantum treatment of the generalized optical Bloch equation for atomic density matrix by a numerical method. In particular, we consider regimes where the light field parameters are beyond the secular approximation (1). Finally, we analyze the width and contrast of localized atomic structures, which are important parameters for technological applications.

II. MASTER EQUATION

Let us consider one-dimensional (along the z axis) motion of atoms with total angular momenta j_g in the ground state and j_e in the excited state in a field of two counterpropagating waves with the same frequency and intensity

$$\mathbf{E}(z,t) = E_0(\mathbf{e}_1 e^{ikz} + \mathbf{e}_2 e^{-ikz})e^{-i\omega t} + \text{c.c.}$$

$$\mathbf{e}_n = \sum_{q=0,\pm1} e_n^q \mathbf{e}_q, \quad n=1,2. \tag{2}$$

Here E_0 is the amplitude of each of the oppositely propagating waves. The unit vectors $\mathbf{e}_1$ and $\mathbf{e}_2$ determine their polarizations with components e_n^q in the spherical basis $\{\mathbf{e}_0=\mathbf{e}_z, \mathbf{e}_{\pm1}=\mp(\mathbf{e}_x \pm i\mathbf{e}_y)/\sqrt{2}\}$.

In this work we restrict our consideration by the weak-field limit where the saturation parameter S is small:

$$S = \frac{\Omega^2}{\delta^2+\gamma^2/4} \ll 1. \tag{3}$$

Here $\Omega=-E_0 d/\hbar$ is the single-beam Rabi frequency, d is the reduced matrix element of the atomic dipole moment.

In the weak-field limit the atomic exited state can be adiabatically eliminated and the atomic evolution is described by the reduced equation for the ground-state density matrix $\hat{\rho}$ [11,12]:

$$\frac{d}{dt}\hat{\rho} = -\frac{i}{\hbar}[\hat{H},\hat{\rho}] + \hat{\Gamma}\{\hat{\rho}\}, \tag{4}$$

where the Hamiltonian $\hat{H}$ is given by

$$\hat{H} = \frac{\hat{p}^2}{2M} + \hbar\delta S\hat{V}^\dagger\hat{V}. \tag{5}$$

The last term in Eq. (5) describes the interaction of atoms with light field in the resonance approximation, where

$$\hat{V} = \hat{V}_1 e^{ikz} + \hat{V}_2 e^{-ikz} = \sum_{q=0,\pm1} \hat{T}_q e_1^q e^{ikz} + \sum_{q=0,\pm1} \hat{T}_q e_2^q e^{-ikz}, \tag{6}$$

and the operator $\hat{T}_q$ is written in terms of the Clebsch-Gordan coefficients

$$\hat{T}_q = \sum_{\mu_e,\mu_g} C^{j_e,\mu_e}_{1,q;j_g,\mu_g} |j_e,\mu_e\rangle\langle j_g,\mu_g|. \tag{7}$$

Here $|j_e,\mu_e\rangle$ and $|j_g,\mu_g\rangle$ are the wave functions of Zeeman sublevels in the exited and ground states, correspondingly.

The relaxation part of master equation (4) has the form

$$\hat{\Gamma}\{\hat{\rho}\} = -\frac{\gamma S}{2}\{\hat{V}^\dagger\hat{V},\hat{\rho}\} + \gamma S \sum_{q=0,\pm1} \int_{-1}^{1} \hat{T}_q^\dagger e^{-iks\hat{z}}\hat{V}\hat{\rho}\hat{V}^\dagger e^{-iks\hat{z}}\hat{T}_q K_q(s)ds, \tag{8}$$

where $\{\hat{a},\hat{c}\}=\hat{a}\hat{c}+\hat{c}\hat{a}$ is the anticommutator and $\hat{z}$ is the position operator. This term describes redistribution of atoms on the ground state Zeeman sublevels due to stimulated absorption and spontaneous emission with taking into account the recoil effects. The functions $K_{\pm1}(s)=(1+s^2)3/8$ and $K_0(s)=(1-s^2)3/4$ are determined by the probability of spontaneous emission of a photon with polarization $q=\pm1,0$ into direction $s=\cos(\theta)$ (relative to the z axis).

III. STEADY-STATE ATOMIC DENSITY MATRIX

There are a number of approaches developed for calculation of the evolution of atomic density matrix. The full quantum treatment is difficult, because it incorporates the evolution of numerous of internal and external degrees of freedom. The majority of works are based on the secular approximation for density matrix elements [11,12,17] as is discussed above. In order to take into account the effects of spatial localization in optical potential more correctly we utilize the full quantum approach for the master equation (4).

In the Wigner representation for atomic density matrix $\hat{\rho}(z,p)$ the master equation (4) takes the following form:

$$\left(\frac{\partial}{\partial t} + \frac{p}{M}\frac{\partial}{\partial z}\right)\hat{\rho}(z,p) = \hat{\gamma}\{\hat{\rho}(z,p)\} - i\delta S[\hat{V}^\dagger\hat{V},\hat{\rho}]^{(W)} - \frac{\gamma S}{2}\{\hat{V}^\dagger\hat{V},\hat{\rho}(z,p)\}^{(W)}. \tag{9}$$

The operator $\hat{V}^\dagger\hat{V}$ in Eqs. (5) and (8) has only the zeroth and second spatial harmonics:

$$\hat{V}^{\dagger}\hat{V} = \hat{W}_0 + \hat{W}_+ e^{i2kz} + \hat{W}_- e^{-i2kz}. \tag{10}$$

Thus, the commutator $[\ldots,\ldots]^{(\mathcal{W})}$ and anticommutator $\{\ldots,\ldots\}^{(\mathcal{W})}$ in the Wigner representation in Eq. (9) are written as

$$\begin{aligned}(\hat{V}^{\dagger}\hat{V}\hat{\rho} \mp \hat{\rho}\hat{V}^{\dagger}\hat{V})^{(\mathcal{W})} &= \hat{W}_0\hat{\rho}(z,p) \mp \hat{\rho}(z,p)\hat{W}_0 + [\hat{W}_-\hat{\rho}(z,p+\hbar k) \\ &\mp \hat{\rho}(z,p-\hbar k)\hat{W}_-]e^{-i2kz} + [\hat{W}_+\hat{\rho}(z,p-\hbar k) \\ &\mp \hat{\rho}(z,p+\hbar k)\hat{W}_+]e^{i2kz}. \end{aligned} \tag{11}$$

The term $\hat{\gamma}\{\hat{\rho}(z,p)\}$ in Eq. (9), describing the spontaneous recoil effect, has the form

$$\begin{aligned}\hat{\gamma}\{\hat{\rho}(z,p)\} = \gamma S \sum_{q=0,\pm1} \int_{-\hbar k}^{\hbar k} \frac{dp'}{\hbar k} K_q\left(\frac{dp'}{\hbar k}\right) \\ \times \hat{T}_q^{\dagger}[\hat{V}_1\hat{\rho}(z,p+p')\hat{V}_2^{\dagger}e^{i2kz} + \hat{V}_2\hat{\rho}(z,p+p') \\ \times \hat{V}_1^{\dagger}e^{-i2kz} + \hat{V}_1\hat{\rho}(z,p+p'-\hbar k)\hat{V}_1^{\dagger} \\ + \hat{V}_2\hat{\rho}(z,p+p'+\hbar k)\hat{V}_2^{\dagger}]\hat{T}_q. \end{aligned} \tag{12}$$

Equation (9) admits a solution that is periodic in the position variable z. We expand the atomic density matrix in Fourier series in the spatial coordinate

$$\hat{\rho}(z,p) = \sum_n \hat{\rho}^{(n)}(p)e^{i2nkz}. \tag{13}$$

From the master equation (9) we have the following recurrence equations for the Fourier components of density matrix $\hat{\rho}^{(n)}$

$$\left(\frac{\partial}{\partial t} + 2ni\frac{p}{M}\right)\hat{\rho}^{(n)} = \mathcal{L}_0\{\hat{\rho}^{(n)}\} + \mathcal{L}_+\{\hat{\rho}^{(n-1)}\} + \mathcal{L}_-\{\hat{\rho}^{(n+1)}\}, \tag{14}$$

where $\mathcal{L}_{0,\pm1}$ are some linear superoperators. Their explicit forms can be derived from Eq. (9) with account for Eqs. (11) and (12).

The steady-state solution $(\partial/\partial t\hat{\rho}^{(n)}=0)$ of this recurrence equations can be obtained by the continued fraction method. This method is a powerful mathematical tool, which is used in a number of physical problems. For example, it was used for solution of the optical Bloch equations in various spectroscopy tasks [19–21] as well as for the calculation of the light force on atom (see, for example, Refs. [22,23]). The major distinction here is that equations (14) for the density matrix contain the recoil effects that makes them more complicated. Note, similar equations were used in Ref. [24], where the authors analyzed the laser cooling (velocity distribution) of two-level atom in the recoil limit (where $\gamma \leqslant \omega_R$), but they restricted the consideration by the lowest spatial harmonics for the density matrix. In other words, the spatial localization was completely neglected in Ref. [24]. In our case the number of spatial harmonics taken into account depends on the light field and atomic parameters. Typically, we use less than 30 harmonics that is enough to obtain the steady-state density matrix in considered range of parameters.

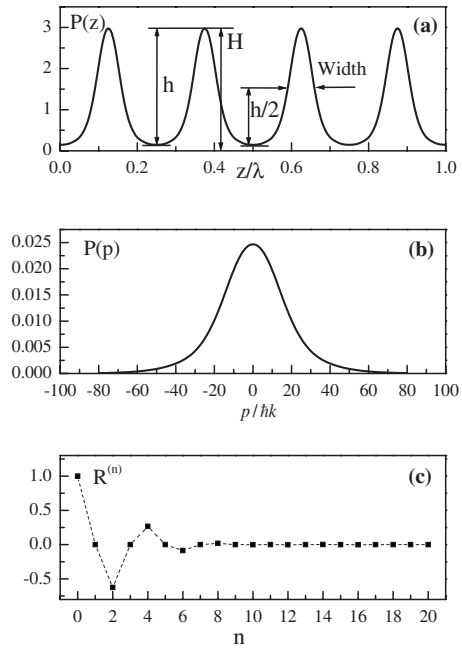

FIG. 1. Steady-state spatial (a) and momentum (b) distributions, and the spatial harmonics of the total population (c) for atoms with $j_g=1\rightarrow j_e=2$ and optical transition and mass corresponding to Cr atoms. The light field detuning $\delta=-40\gamma$ and saturation parameter $S=0.5$.

The spatial and momentum steady-state distributions of atoms with $j_g=1\rightarrow j_e=2$ optical transition for $\delta=-40\gamma$, $S=0.5$ and chromium mass in lin$\perp$lin light field configuration (i.e., the configuration, created by counterpropagating beams linearly polarized with polarizations orthogonal to each other) are shown in Figs. 1(a) and 1(b). The spatial atomic distribution can be characterized by two basic parameters: the full width at half maximum (FWHM) and the contrast which can be defined as the ratio of spatial distribution modulation depth to its amplitude $C=h/H$ [see in Fig. 1(a)] [1]. Figure 1(c) represents the amplitudes of spatial harmonics of the total population $R^{(n)}=\int \mathrm{Tr}\{\hat{\rho}^{(n)}(p)\}dp$. The zeroth

TABLE I. Dimmensionless atomic mass parameter corresponding to optical transitions for different elements suitable for laser cooling.

Element	Cooling transition	λ (nm)	$\tilde{M}$
^{7}Li	$2^2S_{1/2}\rightarrow 2^2P_{3/2}$	671	46
^{23}Na	$3^2S_{1/2}\rightarrow 3^2P_{3/2}$	589	198
^{39}K	$4^2S_{1/2}\rightarrow 4^2P_{3/2}$	766	358
^{85}Rb	$5^2S_{1/2}\rightarrow 5^2P_{3/2}$	780	770
^{133}Cs	$6^2S_{1/2}\rightarrow 6^2P_{3/2}$	852.3	1270
^{52}Cr	$4^7S_3\rightarrow 4^7P_4$	425.6	115
^{27}Al	$3p^2P_{3/2}\rightarrow 3d^2D_{5/2}$	309.4	85
^{69}Ga	$4p^2P_{3/2}\rightarrow 4d^2D_{5/2}$	294.4	382
^{115}In	$5p^2P_{3/2}\rightarrow 5d^2D_{5/2}$	325.7	634
^{107}Ag	$5^2S_{1/2}\rightarrow 5^2P_{3/2}$	328	601

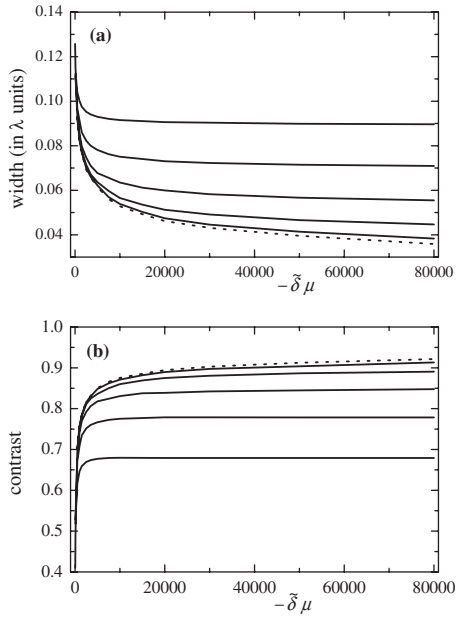

FIG. 2. The spatial width (FWHM) of localized atomic structures (a), and contrast (b) as a function of parameters $\tilde{\delta}\mu$ for different field detunings [solid lines $\tilde{\delta}=-5,-10,-20,-40,-80$ from top to bottom in (a) and from bottom to top in (b)] for optical transition $j_g=1/2\rightarrow j_e=3/2$. The dashed lines corresponds to secular approximation limit.

harmonic is equal to 1 due to the normalization condition. As is seen, the higher harmonics rapidly decrease with number n.

IV. RESULTS

In this section we turn our attention to the steady-state spatial distribution of atoms in the optical potential created by the light field with the lin $\perp$ lin configuration. We choose this configuration as a bright example of the light field with spatially nonuniform polarization. Here only the light field ellipticity varies in the position space, while the other parameters (intensity, phase, orientation of polarization vector) are constant. Moreover, the optical potential created by this configuration has a period of $\lambda/4$ that makes it very attractive for deposition of atomic structures with a high spatial periodicity.

There are several fixed atomic parameters that characterize a given laser cooling situation. These are the atomic mass M, the wavelength λ, and the natural linewidth γ. In addition, there are two parameters that can be varied in experiment: the detuning δ and the saturation parameter S. We use reduced dimensionless units where $\hbar=1$, $k=1$, $\gamma=1$. In this units the dimensionless atomic mass $\tilde{M}$ is defined from the relation $\gamma/\omega_R=2\tilde{M}$ [6]. This is the so-called quasiclassical parameter that characterizes the atomic kinetics in a light field. In particular, it governs the rate of kinetic processes, so that the typical cooling time is of order of $\tau=\omega_R/(\gamma S)$.

As it can be shown directly from Eq. (9), there are only two dimensionless parameters that characterize the steady-state atomic density matrix: the detuning $\tilde{\delta}=\delta/\gamma$ and the parameter μ

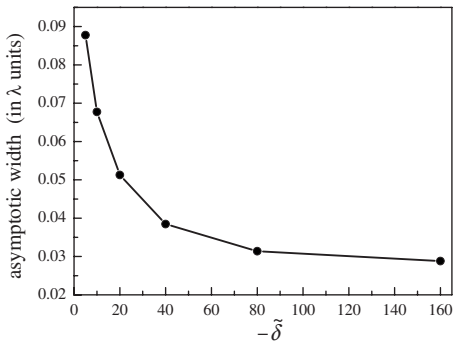

FIG. 3. Asymptotic FWHM of localized atomic structures as a function of the light field detuning for optical transition $j_g=1/2\rightarrow j_e=3/2$.

$$\mu = S\tilde{M}. \tag{15}$$

Thus, the procedure and result of calculations are universal for all atoms with a given angular momentum of energy levels (Table I). First of all, we consider the simple atomic optical transition $j_g=1/2\rightarrow j_e=3/2$ that is utilized in many theoretical works (see, for example, Refs. [9–12,15–17]). The results for the atomic localization and contrast are shown in Fig. 2. Note, that in the secular approximation [15] the stationary solution is characterized only by the ratio of

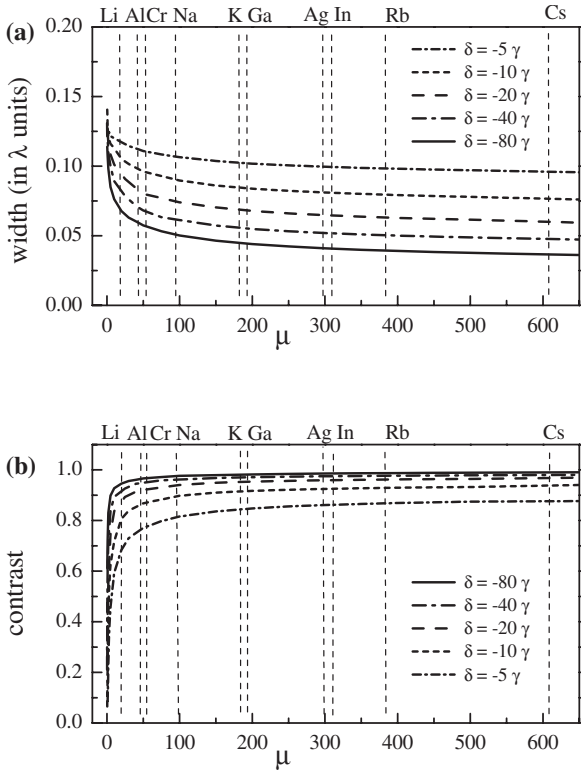

FIG. 4. FWHM of localized atomic structures (a) and contrast (b) as functions of parameter μ for different field detuning for optical transition $j_g=1\rightarrow j_e=2$.

optical potential depth to recoil energy U_0/ω_R, which is proportional to $\tilde{\delta}\mu$ in our notations. In order to compare the secular approximation with exact quantum calculations we express the results in terms of parameters $\tilde{\delta}$ and $\tilde{\delta}\mu$. The dashed lines in Fig. 2 correspond to secular approximation limit. The different solid curves correspond to our results obtained for different detunings in the full quantum treatment. As is seen, the differences between them become more significant with the optical potential depth U_0 increasing, corresponding to violation of secular approximation.

The major difference from secular approximation here is that the width of the localized structures and contrast tend to asymptotic values with increasing of the light field potential depth ($|\tilde{\delta}\mu| \to \infty$). However, this values depend on the light field detuning. The results for the asymptotic values FWHM are shown in Fig. 3.

Additionally, we consider here the more complex optical transition $j_g=1 \to j_e=2$. Apart from the ground state sublevels it incorporates the evolution of coherence of the ground state density matrix. Figure 4 represents the FWHM and the contrast of the spatial structures as a function of parameter μ at different detunings for optical transition $j_g=1 \to j_e=2$. The width monotone decrease for large $\tilde{\delta}$ and μ. In spite of the fact that the equilibrium temperature is growing with the depth of optical potential, the localization of the atoms becomes stronger. Additionally, the contrast tends towards its maximum value, Fig. 4(b). The dashed vertical lines in Fig. 4 show the limitations of the weak-field theory for different elements from the Table I in assumption $S<0.5$ (i.e., these lines correspond saturation $S=0.5$). Note, that this is qualitative estimations for weak-field limits. For thorough definition of these limits the solution of the quantum equation for the total atomic density matrix is required with taking into account the saturation effects. However, the width and the contrast have a very strong dependencies on μ, thus the localization effects remain rather significant for enough small saturation parameter especially for "heavy" atoms (see Table I).

V. CONCLUSION

We performed the full quantum treatment of the atomic localization effects due to laser cooling in a low-intensity with polarization low-intensity light field. Generally, the conditions for a deep laser cooling mismatch the conditions for a strong atomic localization, that requires a deeper optical potential and consequently leads to higher temperatures. Additionally, in a deep optical potential the secular approximation (1) is restricted by the relation on the light field detuning and optical potential depth. In our treatment we had no such limitations. It allows one to describe the atomic spatial distribution more correctly, taking into account localized as well as above-barrier motioned atoms. The steady-state atomic density matrix is a function of the light field detuning δ and the dimensionless parameter μ (15). We analyzed the width and the contrast of localized atomic structures as functions of these parameters. We showed that the width and the contrast have a strong dependence on μ and tend to constant values, depending on the light field detuning, with an increase of the optical potential depth.

We demonstrated the applicability of laser cooling in a far-off detuned deep optical potential, created by a light field with polarization gradient, for the purposes of atom lithography and nanofabrication, suitable for generation of spatially localized atomic features with high contrast. This type of dissipative light masks can be considered as an alternative method for creation of spatially localized atomic structures. The remarkable distinction of this method from nondissipative light masks is that the suggested one is not sensitive to any aberration effects. Moreover, this type of optical masks has no classical analog and cannot be described by the methods of classical optics. Here the width and the contrast of localized atomic structures are determined by the atomic energy dissipation mechanisms in a light field. Finally, we analyzed the possible limits for the width and the contrast that can be reached, in principle, by this type of the light masks.

ACKNOWLEDGMENTS

This work was partially supported by RFBR (Grants Nos. 07-02-01230, 05-02-17086, 04-02-16488, 05-08-01389), by Presidium of SB RAS, and O.N.P. was supported by Grant No. MK-1438.2005.2.

[1] D. Meschede and H. Metcalf, J. Phys. D **36**, R17 (2003).
[2] M. K. Oberthaler and T. Pfau, J. Phys.: Condens. Matter **15**, R233 (2003).
[3] J. J. McClelland and M. R. Scheinfein, J. Opt. Soc. Am. B **8**, 1974 (1991).
[4] Q. Li, K. G. H. Baldwin, H. -A. Bachor, and D. E. McClelland, J. Opt. Soc. Am. B **13**, 257 (1996).
[5] A. P. Kazantsev, G. I. Surdutovich, and V. P. Yakovlev, *The Mechanical Action of Light on Atoms* (Nauka, Moscow, 1991).
[6] R. Stutzle, D. Jurgens, A. Habenicht, M. K. Oberthaler, J. Opt. B: Quantum Semiclassical Opt. **5**, S164 (2003).
[7] O. N. Prudnikov and E. Arimondo, J. Opt. Soc. Am. B **6**, 336 (2004).
[8] D. J. Wineland and Wayne M. Itano, Phys. Rev. A **20**, 1521 (1979).
[9] J. Dalibard and C. Cohen-Tannoudji, J. Opt. Soc. Am. B **6**, 2023 (1989).
[10] S. M. Yoo and J. Javanainen, Phys. Rev. A **45**, 3071 (1992).
[11] J. Guo and P. R. Berman, Phys. Rev. A **48**, 3225 (1993).
[12] Y. Castin, K. Berg-Sorensen, J. Dalibard, and K. Molmer, Phys. Rev. A **50**, 5092 (1994).
[13] P. S. Jessen, C. Gerz, P. D. Lett, W. D. Phillips, S. L. Rolston, R. J. C. Spreeuw, and C. I. Westbrook, Phys. Rev. Lett. **69**, 49 (1992).
[14] P. Verkerk, B. Lounis, C. Salomon, C. Cohen-Tannoudji, J.-Y. Courtois, and G. Grynberg, Phys. Rev. Lett. **68**, 3861 (1992).

[15] Y. Castin and J. Dalibard, Europhys. Lett. **14**, 761 (1991).
[16] K. Berg-Sorensen, Y. Castin, K. Molmer and J. Dalibard, Europhys. Lett. **22**, 663 (1993).
[17] I. H. Deutsch, J. Grondalski, and P. M. Alsing, Phys. Rev. A **56**, R1705 (1997).
[18] S. Marksteiner, R. Walser, P. Marte, and P. Zoller, Appl. Phys. B **60**, 145 (1995).
[19] B. J. Feldman and M. S. Feld, Phys. Rev. A **5**, 899 (1972).
[20] S. Stenholm, Phys. Rep., Phys. Lett. **43**, 151 (1978).
[21] S. A. Babin, D. V. Churkin, E. V. Podivilov, V. V. Potapov, and D. A. Shapiro Phys. Rev. A **67**, 043808 (2003).
[22] V. G. Minogin and O. T. Serimaa, Opt. Commun. **3**, 373 (1979).
[23] S. M. Tan, J. Opt. B: Quantum Semiclassical Opt. **1**, 424 (1999).
[24] S. M. Yoo and J. Javanainen, J. Opt. Soc. Am. B **8**, 1341 (1991).